Simulating the environment at the helicopter-ship dynamic interface: research, development and application

S. J. Hodge
steve.hodge@baesystems.com
Simulation Department
BAE Systems
Lancashire, UK

J. S. Forrest
PRISM Defence
Adelaide, Australia

G. D. Padfield
School of Engineering
University of Liverpool
Liverpool, UK

I. Owen
School of Engineering
University of Lincoln
Lincoln, UK

ABSTRACT

This paper presents highlights from research conducted at the University of Liverpool to determine suitable fidelity criteria and guidelines for the modelling and simulation of the helicopter-ship dynamic interface environment. The paper begins by describing the characteristics of the helicopter-ship dynamic interface, explaining the motivation behind the research and reviewing the state-of-the-art in dynamic interface simulation. The development of a dynamic interface research environment based on an existing research simulator operated by the University of Liverpool is then described, before key results from a number of piloted simulation experiments are presented. These experiments were specifically designed to address fidelity sensitivity issues, such as, are unsteady airwake models necessary, or can a steady airwake model induce appropriate levels of pilot workload? What influence does the modelled ship geometry, or choice of atmospheric wind conditions have on the airwake model and on pilot workload? Finally, the paper concludes by briefly describing the relevance of these research findings to current and future industry programmes.

Paper No. 3760. Manuscript received 12 August 2011,
revised version received 25 November 2011, accepted 2 March 2012.

NOMENCLATURE

d	characteristic body dimension, m
f	wake shedding frequency, Hz
St	Strouhal number
t	simulation time, s
U_∞	free stream velocity, ms^{-1}
u, v, w	ship airwake longitudinal, lateral and vertical velocity components, ms^{-1}
x, y, z	longitudinal, lateral and vertical displacement from origin of ship reference frame, m

Acronyms

ABL	Air-sea Boundary Layer
ACP	Airload Computation Point
CFD	Computational Fluid Dynamics
DES	Detached Eddy Simulation
DIMSS	Dynamic Interface Modeling and Simulation System
DIPES	Deck Interface Pilot Effort Scale
FOCFT	First-of-Class Flying Trials
JSHIP	Joint Shipboard Helicopter Integration Process
MTE	Mission Task Element
RANS	Reynolds Averaged Navier-Stokes
SAIF	Ship/Air Interface Framework
SFS	Simple Frigate Shape
SHOL	Ship/Helicopter Operating Limits
TTCP	The Technical Cooperation Programme

1.0 INTRODUCTION

Of all the harsh environments in which rotorcraft routinely operate, the maritime environment is arguably the most challenging. Simulation of the maritime environment also places some unique demands upon the fidelity requirements of piloted flight simulators used for design and development, or for pilot training purposes. The environment around the ship is known as the dynamic interface. The word 'dynamic' reflects the volatile and time-varying nature of the conditions faced by both the pilot and helicopter, when operating in close proximity to the ship's flight deck and superstructure. Compared with shore-based operations, the dynamic interface is characterised by increased levels of turbulence, severely degraded visual cues and a restricted and moving landing site. These characteristics have significant implications for the computational methods used to model the dynamic interface environment and on the fidelity of the cues (motion, visual and aural) that are available to the simulator pilot. The modelling difficulties presented by the dynamic interface have been the subject of much research activity across the modelling and simulation community[1-4]. However, despite significant increases in computing power and decades of research, there are still no established fidelity standards developed specifically for dynamic interface simulations. Such standards would be of great value for quantifying the fidelity of simulations used for applications such as pilot training, supporting design decisions during the development of new helicopter or ship types and, perhaps most importantly, for the qualification and expansion of safe operating envelopes for existing helicopter and ship combinations. The aim

https://doi.org/10.1017/S0001924000007545 Published online by Cambridge University Press

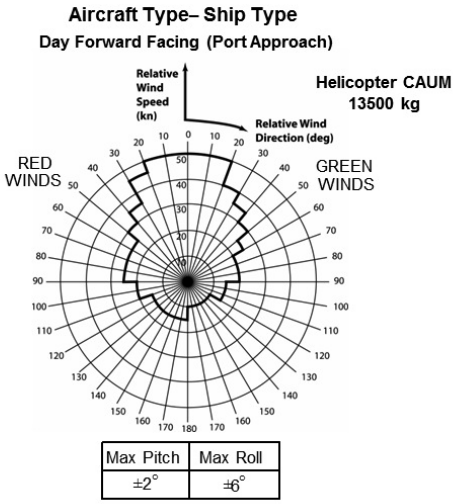

Figure 1. An example of ship/helicopter operating limits.

of the research reported in this paper is to address this shortfall, by providing guidance to those involved in the development and use of helicopter-ship dynamic interface simulations.

2.0 CURRENT PRACTICE

Embarked helicopter operations are conducted within a set of strictly regulated operational boundaries, known as the Ship/Helicopter Operating Limits, or SHOL. In the UK, SHOLs are derived through a qualification process known as 'First-of-Class Flying Trials' (FOCFT), which consists of a series of at-sea flight trials. An example SHOL is given in Fig. 1, where the boundaries of safe operation, for a particular helicopter/ship combination, are expressed in terms of wind speed and direction relative to the ship. Additional information available on the SHOL are the deck motion limits, the landing technique, the helicopter's Corrected All-Up Mass (CAUM) and, in the case of ships which have a large multi-spot flight deck, the landing spot to which the SHOL applies[5]. The CAUM of the helicopter is calculated by correcting the actual aircraft mass to cater for differences in ambient air density to that which was experienced during FOCFT, thereby ensuring that the same power and control margins are experienced in service. In Fig. 1 the term 'Red winds' signify winds from the port side of the ship and 'Green winds' are from the starboard side. For example, a Green 30°/30kt wind refers to a 30kt wind coming from 30° off the starboard side of the ship's bow. During take-off and landing manoeuvres the wind speed and direction, measured at the ship's anemometer relative to the ship, must be within the boundaries prescribed by the SHOL. The development of a SHOL therefore, forms a crucial element of the introduction into service of any newly developed or recently upgraded helicopter and/or ship.

A typical FOCFT programme will require around three to five weeks of intensive sea trials to develop a SHOL for one helicopter/ship combination[6]. During FOCFT a test pilot will repeatedly perform landings and take-offs from the deck of the ship, starting with relatively benign conditions and building-up to more severe conditions in a progressive and controlled manner, until a limit is reached. Limits are reached where the test pilot considers that the workload required to perform a safe deck landing is beyond that which could be consistently achieved by an 'average' fleet pilot.

https://doi.org/10.1017/S0001924000007545 Published online by Cambridge University Press

A limit can also be defined by aircraft performance considerations. For example, in a strong crosswind the helicopter's tail rotor authority limit may be reached, leaving the pilot with insufficient yaw control to compensate for gusts or to maintain heading relative to the ship[7].

Enough data must be gathered during the FOCFT to determine SHOL envelopes for every deck landing spot, at various aircraft masses and, for the Royal Navy, using three different landing techniques (port and starboard side forward facing, and into wind), in both day and night conditions[8], although some 'read-across' is permitted for certain test conditions (e.g. landings which are considered unacceptable at low mass are assumed to be equally unacceptable at higher masses due to reduced performance)[8,9]. Ultimately, the widest possible operational envelope is desired since the helicopter provides the ship with a means of extending its operating range, by carrying a payload of weapons and sensors to locations remote from the ship or by transporting supplies and personnel to the ship. However, conditions which were not experienced during the FOCFT cannot be included in the SHOL envelope. Therefore, if limits are not found during the sea trials, due to benign weather conditions for example, then the resulting SHOL may be overly conservative. This leads to undue restrictions being placed on helicopter flying operations. In which case further sea trials may be needed to gather additional data, or read-across from SHOL data derived for a similar class of ship may be necessary.

Of course safety is a paramount consideration during FOCFT, since the objectives of the trials are essentially to expose the limits of safe helicopter and ship operation, through the identification of conditions at which the maximum pilot workload, degradations in helicopter flying qualities or peaks in ship motion occur. Safety will be at the forefront of the thoughts of the trials team and test pilots, not only at the planning stage, but throughout the trial, as they develop procedures and progressively explore the flight envelope. The planning and execution of FOCFT is therefore complex, costly and time consuming. The prospect of using flight simulation to augment, or even replace, traditional at-sea testing is clearly an attractive one. The potential benefits include a reduction in the costs and risks associated with 'live' flight trials. Moreover, a simulator could provide a safe, controllable and repeatable environment, where any wind and wave conditions can be presented to the pilot an unlimited number of times; thus potentially reducing the likelihood of developing an overly conservative SHOL. The development of high fidelity dynamic interface simulations has long been an aspiration of many individual organisations and of several international collaborative ventures (e.g. The Technical Cooperation Programme (TTCP))[2]. Such simulations could be used to improve the design of future helicopters and ships, to predict and expand safe operating envelopes and to train pilots. However, the use of modelling and simulation in all these applications must be underpinned by a better understanding of the influence of simulation fidelity on pilot behaviour, in terms of their ability to carry out the flying task realistically. Therefore, a key challenge is to develop fidelity criteria specifically tailored for helicopter-ship dynamic interface applications.

3.0 SIMULATION FIDELITY

The initial challenge that must be faced when defining new fidelity criteria, for any application, is the lack of a common understanding of what simulation fidelity actually entails. This question has been the source of intense research and debate over several years, but despite this attention there is still no single, agreed, definition of simulation fidelity. A common theme however, used in many studies, is to make a distinction between those characteristics of a simulator which can be measured objectively, and those which the pilot experiences subjectively. Barnes[10] groups these two sets of distinct but highly interrelated characteristics under the headings of 'accuracy' and 'realism'.

https://doi.org/10.1017/S0001924000007545 Published online by Cambridge University Press

An accurate simulation will have a high level of objective, or engineering, fidelity. Objective fidelity is described as the degree to which the simulation reproduces measurable aircraft or environmental states, as sensed or recorded by non-physiological instrumentation onboard the simulator[11]. The accuracy of a simulator can therefore, in principle, be comprehensively measured through direct comparison of the recorded simulator characteristics, or response, with available sources of real-world test data.

The second category of fidelity, subjective fidelity, is defined as the degree to which simulator participants subjectively perceive the simulation to be representative of the real-world. This type of fidelity is, by its very nature, not as easily measured or as completely understood as objective fidelity. Subjective fidelity is pilot-centred and includes both physiological and psychological effects[11]. Moreover, subjective fidelity is not guaranteed by simply assembling a simulation from several highly accurate models or highly capable components (i.e. motion, visual and audio cueing devices).

A useful holistic definition of fidelity, given by Hess and Siwakosit[12], relates simulation fidelity to pilot behaviour, and states that 'Simulation fidelity can be described as the degree to which characteristics of perceivable states induce adequate psychomotor and cognitive behaviour for a given task and environment'. This definition introduces the concept that simulation fidelity is a relative term, which is only meaningful in the context of a specific task and, therefore, the level of fidelity appropriate for one particular task may not necessarily be applicable to another. Moreover, the concept is introduced that not only the piloting task, but also the simulated environment in which the task is being performed, has significant implications on the fidelity requirements of the simulation.

Bray[13] extends this argument by stating that 'Subjective fidelity or a sense of realism in the flight simulator is essential to productive use in research or training. Depending on the nature of the simulated flight task and the objectives of its use, varying degrees of objective, or engineering, similarity to the flight situation are required to create that realism'. This definition supports the view that existing simulation fidelity standards, such as those developed for use in the qualification of pilot training simulators[14], will not necessarily be applicable to simulators used for predicting SHOL envelopes.

The answer to the question – 'How much fidelity is required?' in any particular situation is therefore dependent upon the simulated task, the environment in which the task is performed and, above all, on the purpose of the simulation. For example, a high fidelity cockpit simulation is required to provide a realistic environment in which to train fleet pilots. On the other hand, pilots who take part in FOCFT are very experienced and may not require that level of realism in what is essentially an 'eyes-out-of-the-window' task[15]. However, if SHOL envelopes are to be predicted in a flight simulator then accurate models of the helicopter-ship dynamic interface will be essential. A typical high fidelity dynamic interface simulation includes accurate mathematical models of the helicopter, the disturbed airflow around the ship (known as the ship's airwake) and the ship's motion. The latter will be combined with realistic visual models of the ship and ocean surface, and all of these will be integrated with a representative cockpit mounted on a six degree-of-freedom motion platform to provide body force cues to the pilot. The interactions between these models and cueing systems, which might individually be of a very high fidelity, must also be carefully considered. An important step in developing fidelity criteria, for the helicopter-ship dynamic interface, is to build such a simulation, populate it with models and subsystems of varying fidelity, and then use the simulation to carry out fidelity sensitivity studies. This process is described later in the paper; but first, a selection of literature is briefly reviewed to establish the state-of-the-art in dynamic interface simulation and place the current research into context.

4.0 DYNAMIC INTERFACE SIMULATION RESEARCH

Woodfield and Tomlinson[1] have described the development of an empirical model of the airflow around a Type 23 frigate. This model used superposition of various generic components, which are typical of the large-scale flow features found in the lee of bluff bodies (e.g. a ship's hangar), to model the whole flow field. Later, Tate[6] described how this model was integrated into the Advanced Flight Simulator (AFS) at DERA (now QinetiQ) in the UK, for use in piloted evaluations, and reports that the main criticism was the absence of any turbulence effects.

At the same time in the US, the requirement for high fidelity simulations to prepare pilots for shipboard flight testing of the V-22 Osprey tilt-rotor was dictating the pace of progress. Reddy[16] describes several enhancements made to the Manned Flight Simulator (MFS) facility at the Naval Air Warfare (NAVAIR) test centre, Patuxent River. These updates to an existing high fidelity V-22 simulation included a new ship airwake model which employed a combination of data derived from steady-state Computational Fluid Dynamics (CFD) simulations and empirical turbulence models; a ship motion model using data recorded from a ship at sea; and various improvements to the simulator's outside-world visual scene.

During the period covering 2000 to 2002, a number of publications emerged reporting progress on the Dynamic Interface Modeling and Simulation System (DIMSS) element of the US Navy's Joint Shipboard Helicopter Integration Process (JSHIP)[15,17]. The JSHIP program was established to increase the interoperability of joint helicopter operations (including Navy, Marines, Air Force, Army and Coast Guard helicopters) from Navy ships. The goal of DIMSS was to support this interoperability by defining and validating a process for developing launch and recovery envelopes (i.e. SHOLs) using high fidelity simulation. Bunnell[18] describes how, as part of the DIMSS effort, a blade-element model of a UH-60 helicopter[19] was integrated with a time-accurate model of an LHA class ship airwake[3]. The development of the time-accurate airwake model was made possible by the use of advanced CFD techniques and high-performance parallel-computing. The host facility used for the simulation was the NASA Ames Vertical Motion Simulator (VMS), which is the largest motion-base research simulator in the world[17]. Despite the progress made, the DIMSS ultimately fell short of its intended goal of a fully validated and accredited process, due to a lack of suitable validation data.

The UK MoD funded Ship/Air Interface Framework (SAIF) was first established in 2003 with the aim of developing the capability to accurately predict SHOLs for aircraft operating from the Royal Navy's Type 45 destroyer and other future UK warships. The SAIF program host facility is the Merlin training simulator at the Royal Naval Air Station (RNAS) at Culdrose. Cox *et al*[20] describe how the flight simulator at Culdrose was modified with a distributed and federated structure, based on the industry-standard High Level Architecture (HLA). This modification allows individual components, such as the ship airwake and ship motion models, to be replaced for experimentation purposes, with minimal disruption to the facility's core role of pilot training. The SAIF programme is seen as a key tool for de-risking the design, development and entry into service of future Royal Navy vessels.

Previous studies, like those described above, have made some simplifying assumptions in order to make real-time simulation of the helicopter-ship dynamic interface a feasible proposition. These assumptions in most cases include: (i) Neglecting the time-varying component of the ship's airwake, (ii) Assuming that the ship airwake is not affected by the motion of the ship, (iii) Neglecting the effects of atmospheric turbulence and the atmospheric boundary layer and (iv) Assuming a one-way coupling between the ship and helicopter, so that the presence of the helicopter and rotor downwash has no influence on the ship's airwake. Recent advances have

https://doi.org/10.1017/S0001924000007545 Published online by Cambridge University Press

concentrated on fully-coupled helicopter flight dynamics and CFD ship airwake simulations, as well as modelling the airwake of a moving ship. The former has been accomplished by tight integration of helicopter flight dynamics models with CFD simulations of ship airwake; the latter by using CFD simulations with dynamically moving meshes. The computational power required in both of these approaches means that they are presently not viable for use in real-time simulations. For example, Bridges *et al*[21]describes a non-realtime fully-coupled helicopter/ship simulation which integrated a high-fidelity helicopter flight dynamics model with a CFD ship airwake simulation and employed a mathematical model to predict pilot workload. The results showed that the one-way coupling method, currently employed in all real-time simulations, predicted a level of pilot workload similar to that of the fully-coupled method using the same pilot model.

The current research is focused on real-time simulation of the helicopter-ship dynamic interface, so must invoke the one-way coupling assumption. In addition, the assumption that the airwake is not affected by ship motion is also made. Nevertheless, this research does make significant advances in modelling the time-varying component of the ship's airwake and the atmospheric boundary layer over the sea. The one-way coupling assumption is clearly a simplification compared to the actual coupled helicopter-ship situation, but the advantage is that real-time flight simulation allows for opinion to be gathered from an experienced test pilot, rather than a theoretical pilot model.

5.0 DYNAMIC INTERFACE MODELLING AND SIMULATION

This section briefly describes the various models and components that comprise the helicopter-ship dynamic interface simulation which has been developed as part of this research, with particular emphasis on the fidelity requirements of each model. The concluding part of this section describes the integration of these model components into an integrated dynamic interface simulation.

5.1 Flight simulation facility

The flight simulation facility used for the current research is the HELIFLIGHT-R simulator, operated by the University of Liverpool[22]. The HELIFLIGHT-R is a fully reconfigurable research simulator, consisting of a generic rotorcraft cockpit housed inside a 12ft diameter visual display dome, mounted on a motion platform (Fig. 2(a)). The motion platform is of the standard hexapod configuration, comprising six electric actuators each with a 24 inch stroke[23]. The simulator cabin houses a twin-seat cockpit, with a third seat at the rear for an instructor or simulator operator (Fig. 2(b)). The primary cockpit instruments are presented on two wide-screen flat-panel displays. A four-axis electronic control loading system provides the capability to configure the force-feel characteristics of both the pilot and co-pilot's cyclic, collective and pedal controls to represent a wide range of aircraft types. Three Liquid Crystal on Silicon (LCoS) projectors, with a resolution of 1,400 by 1,050 pixels, are used to project an outside-world image onto the inside surface of the dome. The three images are geometry-corrected and edge-blended, before being projected, so as to present a single continuous image to the pilot in the cockpit. The projectors are equipped with wide-angle lenses and provide a horizontal field-of-view of 200° (±100°) and a vertical field-of-view of 60° (±30°). Audio cues are presented to the pilot using a system of loudspeakers distributed throughout the interior of the cockpit.

https://doi.org/10.1017/S0001924000007545 Published online by Cambridge University Press

Figure 2. The HELIFLIGHT-R simulator; (a) Motion platform and display dome, (b) Pilot's view of the dynamic interface simulation and cockpit.

5.2 Helicopter flight dynamics model

Helicopter flight dynamics models have been developed in FLIGHTLAB, which is a commercially available software tool that provides a multi-body modelling and simulation environment[24]. By using FLIGHTLAB, complete rotorcraft simulations can be rapidly constructed from a library of pre-defined components[25]. For these experiments a FLIGHTLAB model of a helicopter having a conventional articulated main rotor with four blades, was configured to be representative of a Sikorsky SH-60B Seahawk helicopter. The SH-60B is a maritime helicopter, derived from the ubiquitous UH-60A Black Hawk utility helicopter, which is currently in service with several navies throughout the world. The SH-60B was selected because of the wide availability of engineering data for that type of helicopter in the open literature[19,26].

The FLIGHTLAB model of the SH-60B comprises the following major subsystem components: (1) individual blade-element main-rotor model including look-up tables of non-linear lift, drag and pitching moment coefficients stored as functions of incidence and Mach number; (2) Bailey disk tail-rotor model, (3) finite-state Peters-He dynamic inflow model; (4) separate look-up tables for the fuselage, vertical tail and the port and starboard stabilator forces and moments stored as non-linear functions of incidence and sideslip; (5) turbo-shaft engine model with a rotor-speed governor; (6) primary mechanical flight control system and Stability Augmentation System (SAS) models including sensor and actuator dynamics; and (7) a landing gear model to provide deck reactions cues on touchdown. Padfield[27] describes this level of modelling as medium fidelity, capable of simulating trim and primary-axis responses faithfully. Handling qualities characteristics are also generally well predicted using this type of flight dynamics model.

5.3 Ship airwake model

The disturbed airwake in the lee of a ship is characterised by turbulent eddies, recirculation zones, separated flow, vortices and moving shear layers that combine to buffet the helicopter during flight close to the superstructure (Fig. 3). The prevailing wind conditions have a significant impact on

https://doi.org/10.1017/S0001924000007545 Published online by Cambridge University Press

the nature of the airwake. The wind direction, for example, has a dramatic effect on the structure of the flow field.

In general, a ship's airwake can be considered to be made up of two components; an essentially steady flow pattern, which is dependent on the geometry of the ship and the wind direction, and varies little with time; and a superimposed unsteady component that varies significantly and often rapidly with time. In practice, when related to the SHOL, it is the steady component that causes restrictions due to reduced helicopter thrust and control margins below safe operational limits. The unsteady component, on the other hand, leads to high levels of pilot workload. Moreover, the presence of this unsteady component has profound implications for the type of computational methods that can be used to accurately model the airwake environment.

Some dynamic interface simulations have used data derived from steady-state CFD analysis to develop airwake models which spatially map the flow topology around the ship[16,28,29]. A fundamental problem with this approach is that steady-state models are only capable of capturing stationary gradients in the flow field and, significantly, ignore any temporal or time-varying component. In a simulator, a stationary flow field will demand little in the way of pilot compensation as the helicopter translates through the airwake. In order to model pilot workload with increased fidelity, a time-accurate or unsteady airwake model is required. An unsteady airwake presents the pilot with a time-varying disturbance rejection task, leading to increased control activity and higher pilot workload.

In the current research, ship airwake models were developed using both steady and unsteady CFD for two different ship geometries (Fig. 4). The first geometry is the Simple Frigate Shape (SFS), which was originally developed as a generic model to promote comparison between the numerous CFD simulations and various experimental databases produced by the participating nations of TTCP (Australia, Canada, the United Kingdom and the United States)[2]. The second ship geometry is representative of the Type 23 Duke Class anti-submarine frigate which is currently in service with the Royal Navy and is substantially more detailed than the SFS. The unsteady CFD simulations were performed using Detached Eddy Simulation (DES), which overcomes the limitations of traditional turbulence models (e.g. two-equation Reynolds Averaged Navier-Stokes (RANS) models) by explicitly resolving medium to large-scale turbulent eddies and only modelling small scale turbulence in the near-wall region. The use of DES techniques was largely made possible by the procurement of a High Performance Computing (HPC) cluster. With this step-change in computing power unsteady airwake simulations could be performed in acceptable timescales.

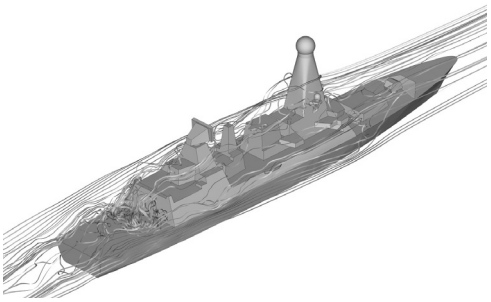

Figure 3. Airwake environment around a single-spot ship.

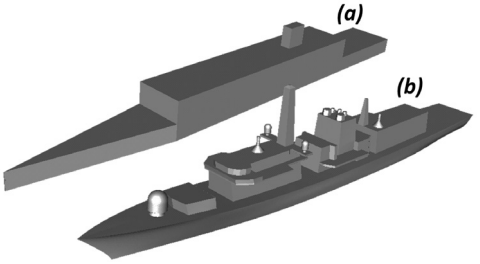

Figure 4. Ship geometries;
(a) Simple Frigate Shape, (b) Type 23 frigate.

https://doi.org/10.1017/S0001924000007545 Published online by Cambridge University Press

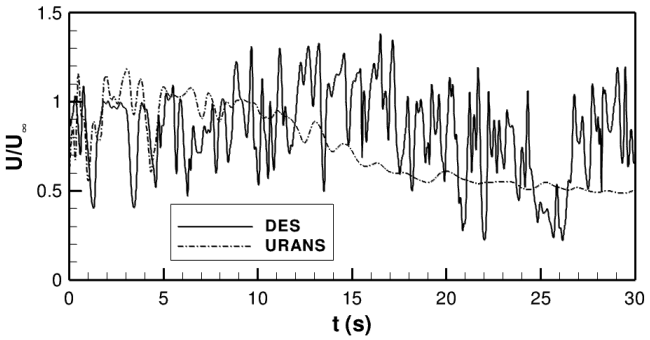

Figure 5. Time history of normalised velocity magnitude at a point in the flow above the SFS flight deck using DES and URANS.

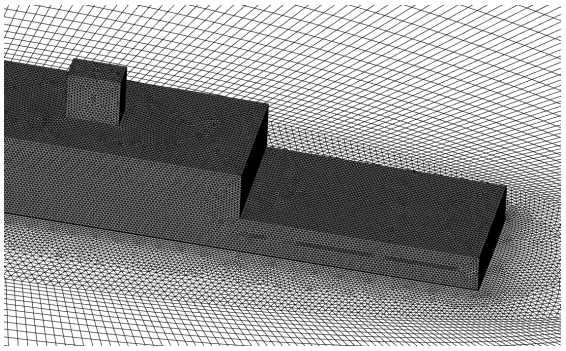

Figure 6. Surface mesh used for the simple frigate shape.

The commercial CFD code, FLUENT, was used for the current study. Second order discretisation was used in time and space, with blended upwind/central differencing scheme used for the convective terms. Pressure-velocity coupling was achieved through the use of the PISO scheme. The approach to turbulence modelling used for the DES simulations was based on the Spalart-Allmaras (S-A) turbulence model. Although the DES turbulence model captured the majority of the airwake turbulence, a background turbulence field was set by specifying an inlet eddy-viscosity equivalent to 10% turbulence intensity. The use of Unsteady RANS (URANS) techniques was initially evaluated as an alternative to DES. However, it was found that URANS computations were unable to resolve the same level of detail as DES and furthermore, that the URANS solutions quickly 'damped-out', or converged, to a steady-state solution (Fig. 5). This convergence back to steady-state conditions is thought to be caused by unrealistically high levels of turbulent eddy-viscosity predicted by the URANS turbulence model.

The ship geometries were placed in domains with dimensions chosen such that blockage effects were negligible, and meshed using an unstructured scheme. The baseline meshes for the SFS (Fig. 6) and Type 23 geometries contained approximately 5·8 million and 6·7 million cells, respectively. A time step of 0·0125 seconds was chosen for the unsteady CFD simulations.

In order to gain confidence in the accuracy of the CFD modelling a validation study was conducted, comparing the results obtained using both ship geometries with experimental data. Validation data for the SFS was obtained from the National Research Council of Canada (NRC) consisting of a comprehensive wind-tunnel database. The UK Defence Science and Technology

https://doi.org/10.1017/S0001924000007545 Published online by Cambridge University Press

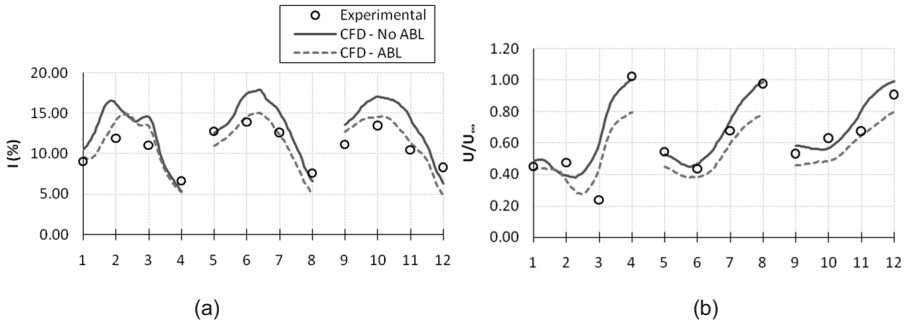

Figure 7. Comparison of Type 23 CFD results with experimental data at anemometer sample points for a green 10° wind; (a) turbulence intensity, (b) normalised velocity magnitude.

Laboratory (dstl) provided anemometer data derived from at-sea tests to validate the Type 23 frigate model. Figure 7 compares the results for the Type 23 frigate simulations with at-sea data, and shows that a good agreement is obtained for both time-averaged turbulence intensity and normalised velocity magnitude, at twelve different locations over the ship's flight deck. In Fig 7 points 1-4 are closest to the hangar face, 9-12 are furthest aft, and 10 and 11 are directly above the landing spot with all points being located at hangar height. It can be seen from Fig. 7 that the CFD model captures the trends in turbulence intensity and velocity magnitude well and, that a significant improvement in the prediction of turbulence can be obtained by applying an Air-Sea Boundary Layer (ABL) profile at the inflow boundary. Further details regarding the development and validation of the ship airwake models can be found in Refs 30 and 31.

5.4 Ship motion model

The motion of a ship in high sea states is a function of the ship's geometry, loading and inertia, and the direction from which the waves approach the ship. In some cases the ship's motion, which causes the flight deck to rotate and translate, may define the limits of the SHOL. Moreover, each SHOL will only be cleared up to the maximum ship motion conditions encountered during the sea trials[32]. The ship motion model used in these experiments was provided by re-playing time history data recorded from a Royal Navy vessel at sea. Although the vessel in question was much larger than a frigate, the time history data was scaled linearly so that the peaks in ship motion matched those typically experience by a frigate sized vessel. The scaling of ship motion data in this manner has been shown to be valid, since wave periods typically remain constant over a range of sea states[33]. The time history data included 20 minutes of deck motion in the roll, pitch, yaw and surge, sway, heave axes, recorded in sea state six conditions with a wave encounter heading of 165° measured from the stern.

An example of the ship motion data in the roll, pitch and heave axes measured at the ship's centre of gravity is shown in Fig. 8, where heave corresponds to vertical motion of the flight deck. The advantage of using real deck motion, recorded at sea, is that it contains realistic quiescent periods which the pilot expects to encounter. Quiescent periods are relatively calm periods of ship motion, which occur naturally, even in high sea states. Pilots will normally elect to hover alongside or over the deck (depending on aircraft agility), assessing the ship's motion and waiting for a suitable period of quiescence before committing to a landing. The disadvantage of this approach is that a large database of time histories, including variations of sea state, ship speed and wave heading will be required to develop SHOL envelopes in a flight simulator.

https://doi.org/10.1017/S0001924000007545 Published online by Cambridge University Press

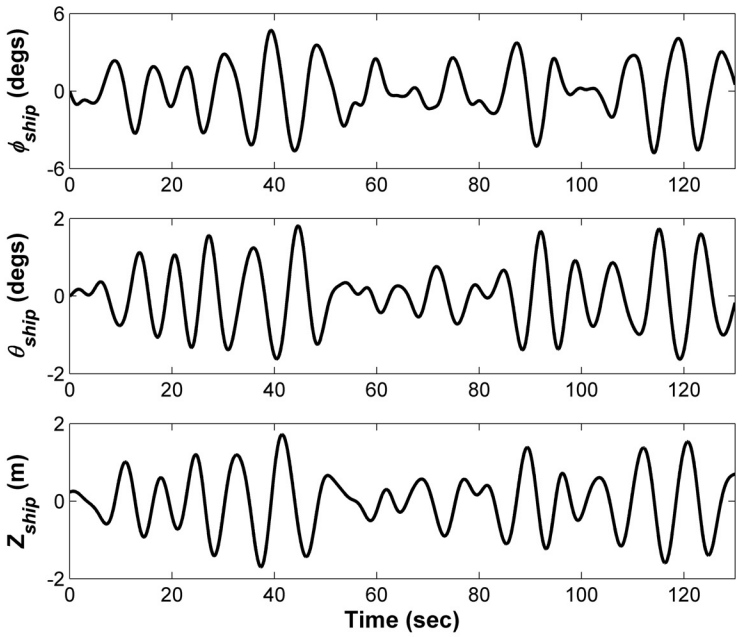

Figure 8. Example of simulated ship motion in sea state six conditions measured at the ship's centre of gravity.

5.5 Sea surface and ship visual models

For these experiments a detailed photo-textured model of the Type 23 frigate was integrated into the simulator's outside-world scene (Fig. 2(b)). The outside-world scene also included a realistic ocean environment with a dynamic sea surface and dynamic water-wake models attached at the bow and stern of the ship. The importance of not only realistic photo-texturing, but also modelling individual key features on the flight deck and superstructure has been demonstrated by previous dynamic interface research[33]. It was therefore, considered important that all of the ship's deck dimensions and markings were accurately modelled. As a result the Type 23 frigate visual model included a Flight Deck Officer (FDO), deck lock grid, horizon bar, antenna masts, cranes, radars, lifeboats and deck netting, together with accurate models of the ship-mounted visual landing aids[34]. Pilots will also make use of visual cues from the surface of the sea to estimate height and to predict ship motion. This means that adequate modelling of the sea surface is particularly important. A fully dynamic sea surface is one which moves in three dimensions and contains realistic peaks and troughs. Tate[6] explains the importance of a dynamic sea representation in helicopter/ship simulations, saying that 'without it the whole picture looks rather 'artificial' because the ship is moving but the sea surface remains flat calm'.

The generation of real-world waves is caused by near-surface winds acting as a stress upon the ocean surface, these so-called 'wind waves' are first generated as ripples and gradually build in height and length as the fetch (i.e. the distance over which the winds have been blowing) increases[35]. Local wind-wave systems can often become mixed with long wavelength swells, induced by winds that have been blowing several kilometres away. This mixing creates a complex wave field where, to an observer, the direction of travel of individual waves can often seem quite unrelated[6]. Like for many naturally occurring phenomena, accurate simulation of the sea surface is a very demanding task, particularly for real-time simulation. Today, most commercial image

https://doi.org/10.1017/S0001924000007545 Published online by Cambridge University Press

generator applications and many PC simulator games provide very realistic simulations of the ocean surface[36]. In the HELIFLIGHT-R simulator however, bespoke image generator software is used and this software has limitations compared to the current state-of-the-art commercial products[37]. Nevertheless, a useful feature that is provided by the existing software is the ability to automatically generate terrain 'on-the-fly'. This feature was exploited to create a simulation of the undulating sea surface. First, a rectangular grid of points was defined on the sea surface around the ship. The vertical height of each grid point was then calculated, at each simulation time step, using a simple 'sum-of-sinusoids' algorithm (i.e. a Fourier series) the sea surface is then rendered and textured. This process is illustrated in Fig. 9 using two orthogonal sine waves. The disadvantage of this approach is that it is computationally expensive and, as a result, only a few sine wave components can be used. Nevertheless, pilot feedback suggests that even a very small number of sinusoids, travelling in the direction of the main wind vector, has the effect of greatly enhancing the realism of the visual scene and the pilot's ability to estimate height. In this simulation it was not possible to correlate the motion of the ship (described in Section 5.4) with the sea surface motion. This naturally denies the pilot the ability to anticipate periods of quiescent ship motion using cues from the sea surface alone. Although this does not appear to have been of particular concern to the pilot, proper correlation of the ship and sea surface models should be considered as an area for further research.

5.6 Model integration

Careful integration of each individual model was required to ensure that the overall fidelity of the simulation was preserved. In this section the steps taken to integrate the helicopter flight dynamics model and the ship airwake model are described.

As described in Section 5.3 the unsteady CFD airwake simulations produced large quantities of time-varying data for each of the three airwake velocity components (*u, v* and *w*), sampled at each point on an unstructured computational mesh, at a rate of 80Hz. The data in this format is unsuitable for direct implementation into a real-time simulation environment. Instead, the data must first be interpolated onto a structured grid, so that it can be stored in look-up tables. Furthermore, in order to reduce the data storage burden, only every fourth time step was used (i.e. the data was down-sampled to 20Hz). Figure 10 shows the structured grid selected for the Type 23 frigate simulations. This structured grid was designed to cover only the near-field region, around the ship, where the helicopter was expected to operate during deck landings. A uniform grid spacing of 1m was selected, because this resolution compares well with the SH-60B main rotor diameter of approximately 16m. To achieve real-time performance, the contents of the look-up table must be stored in the simulation host computer's local memory. This avoids the relatively lengthy process of

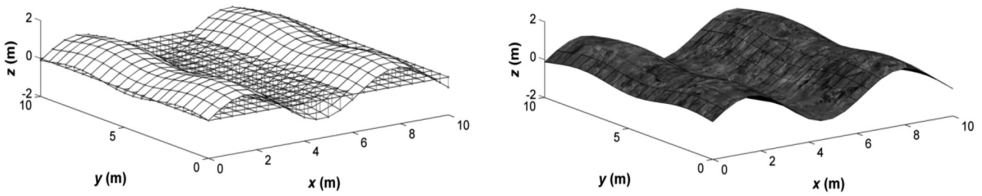

Figure 9. Sea surface simulation using two sine waves;
(a) vertical height of each grid point, (b) final textured surface.

https://doi.org/10.1017/S0001924000007545 Published online by Cambridge University Press

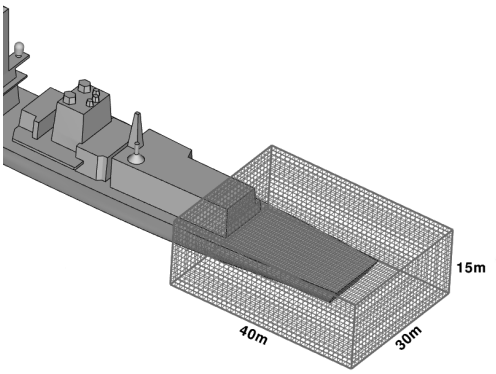

Figure 10. Structured grid used for the Type 23 frigate real-time look-up tables.

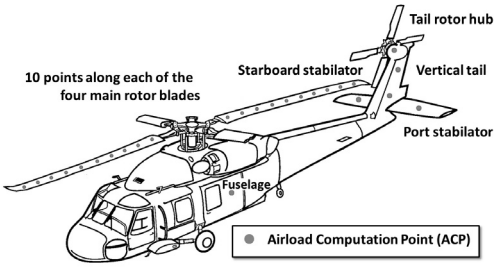

Figure 11. Location of airload computation points on the SH-60B helicopter model.

accessing hard disk storage, but places a practical limitation on the size of look-up table that can be used. In these experiments airwake time histories were limited to approximately 30 seconds. However, since a typical deck landing will normally take longer than 30 seconds, then the time histories were looped smoothly throughout the duration of the manoeuvre. Airwake look-up tables were generated for wind directions of Red 60° through to Green 60° in increments of 15° (including headwinds), as well as for Red 90° and Green 90° winds. In order to maintain real-time execution a pragmatic balance must be struck between the size of the airwake model domain, the sampling frequency and the time history length. For a fixed size of physical memory an increase in any one of these parameters must necessarily mean a reduction in one or more of the remaining parameters. Increasing the available physical memory and hard disk storage capacity will, of course, help to ameliorate these limitations in the near term. However, further research should consider new ways of storing, compressing and interpolating airwake data[38]. For the airwake model to influence the flying qualities of the simulated helicopter, the airwake velocity components must be converted into forces and moments, and applied at the helicopter model's centre of gravity. To accomplish this local airwake velocity components are calculated at a number of Airload Computation Points (ACPs) distributed around the helicopter. A total of 46 ACPs were defined for the SH-60B model (Fig. 11), including one ACP at the centre of each of the ten blade elements on each of the four main rotor blades, one at the tail rotor hub, two on the vertical tail surface, one each on the port and starboard stabilators and one at the aerodynamic centre of the fuselage. During a simulation run, at each time step, the spatial location of every ACP is computed relative to the ship. The resulting offsets (x, y and z) and the current simulation time, t, are then used to extract the local airwake velocity components, at each ACP for the current time step, from the airwake look-up tables using a four-dimensional interpolation algorithm. The airwake velocities are defined in ship axes, so for the fuselage, empennage (stabilators and vertical tail) and tail rotor hub, these velocities must be transformed from the ship reference frame into an inertial frame and then into the helicopter body-fixed reference frame. A further conversion into local rotor blade co-ordinates is required for each ACP on the main rotor blades. To confirm that the airwake model had been properly integrated with the helicopter model, a verification test was carried out. This involved positioning the helicopter model, so that the fuselage ACP was coincident with a pre-defined monitor point in the airwake. The helicopter and ship positions were then 'frozen' to prevent relative motion, by disabling the integration of acceleration, velocity and position, and a real-time simulation was performed over a period of 30 seconds. The resulting airwake components at the fuselage ACP were then compared

https://doi.org/10.1017/S0001924000007545 Published online by Cambridge University Press

with velocity values extracted from the original CFD dataset, at the same monitor point, and the two sets of data were found to be in good agreement.

6.0 EXPERIMENT DESIGN AND CONDUCT

This section discusses the design and conduct of the simulator experiments, including a definition of the deck landing manoeuvre and the subjective rating scales used for eliciting pilot opinion. The parameters needed to define the conditions at the dynamic interface are also explained.

6.1 Deck landing mission

Any mission can be constructed from a contiguous sequence of Mission Task Elements (MTEs), each with distinct start and end conditions, and with defined goals in terms of flight and mission performance. The concept of the MTE was first introduced by the Aeronautical Design Standard (ADS-33) document, which contains descriptions of more than 20 MTEs specifically related to battlefield helicopter operations[39]. The mission of interest in this research is, however, the recovery of a maritime helicopter to the deck of a single-spot ship and the conduct of this mission is highly dependent on a variety of factors including the flying qualities of the helicopter; the disturbed airflow around the ship's superstructure; flight deck motion; the availability of visual cues; and different nations will also employ different recovery procedures (e.g. US Navy technique[40]). Throughout the current research we have adopted, as far as possible, the standard Royal Navy procedure for port-side forward-facing recoveries shown in Fig. 12. By following this technique the pilot guides the helicopter to a stabilised hover on the port side of the ship, then manoeuvres sideways across the deck to re-position over the deck landing spot, and waits for a quiescent period in the ship's motion before landing. Three MTEs were identified from this description of the deck landing mission: (i) Sidestep manoeuvre; (ii) Station keeping (precision hover) above the flight deck; and (iii) Vertical landing. These three elements of the deck landing mission have previously been identified as the most demanding in terms of pilot workload[5,33].

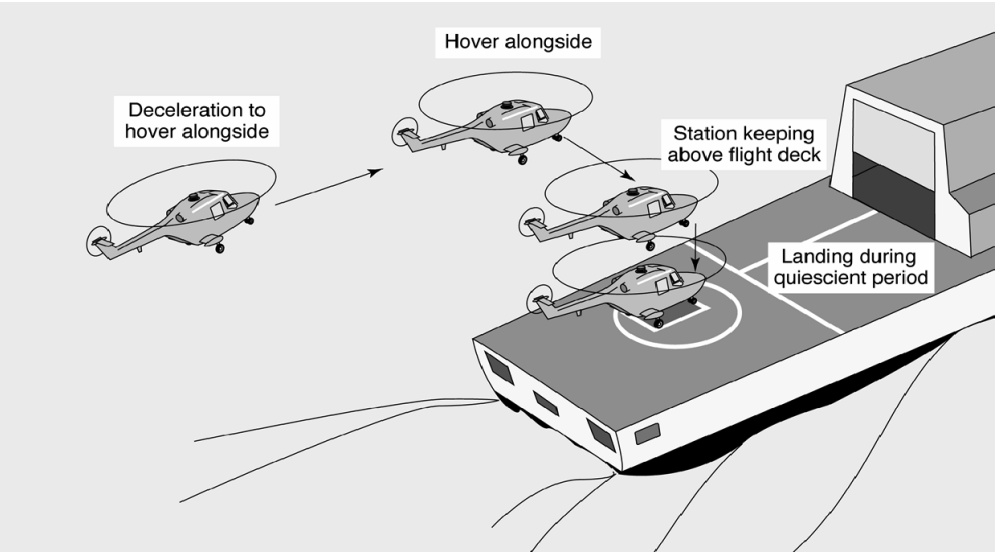

Figure 12. Final stages of the recovery of a Royal Navy helicopter to a single-spot ship.

https://doi.org/10.1017/S0001924000007545 Published online by Cambridge University Press

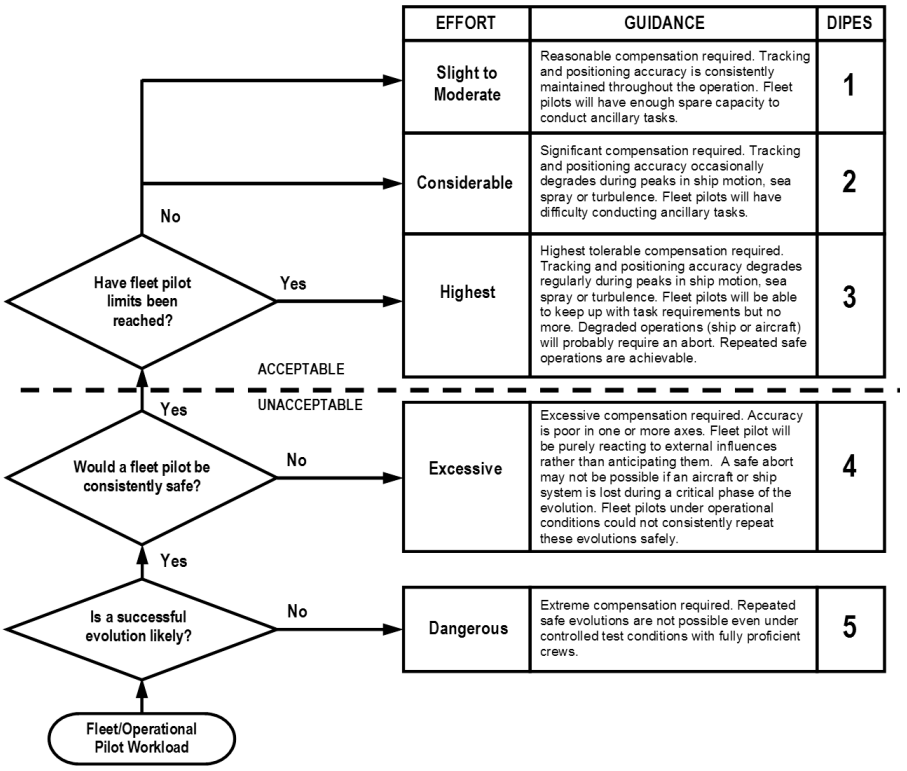

Description	Suffix	Description	Suffix
Pitch control:	P	Height control:	H
Turbulence:	T	Spray:	S
Roll control:	R	F/Aft positioning:	F
Deck motion:	D	Torque control:	Q
Yaw control:	Y	Lateral positioning:	L
Visual cues:	V	Funnel Exhaust:	E
A/C attitude:	A		

Figure 13. Deck interface pilot effort scale.

6.2 Subjective rating scales

The pilot was asked to quantify the workload involved in each deck landing using the same 5-point rating scale that is used during FOCFT (Fig. 13). The Deck Interface Pilot Effort Scale (DIPES)[8] requires the test pilot to rate each landing based on workload (or pilot compensation), performance, accuracy and consistency. On the DIPES scale a numerical rating of 3 or less indicates that deck landings can be repeatedly achieved with precision and safety, under the conditions being tested. A rating of 4 or 5 indicates the contrary and places that condition outside of the SHOL, thus prohibiting deck landings under those conditions. In addition to the detailed comments given by the pilot, a number of letter suffixes can also be assigned to each rating, to describe the cause of increased workload (e.g. 'T' for turbulence or 'D' for deck motion). Of these suffixes, only spray (S) which reduces the pilot's visibility, and funnel exhaust (E) which affects engine performance if ingested, are not currently modelled in the simulator.

https://doi.org/10.1017/S0001924000007545 Published online by Cambridge University Press

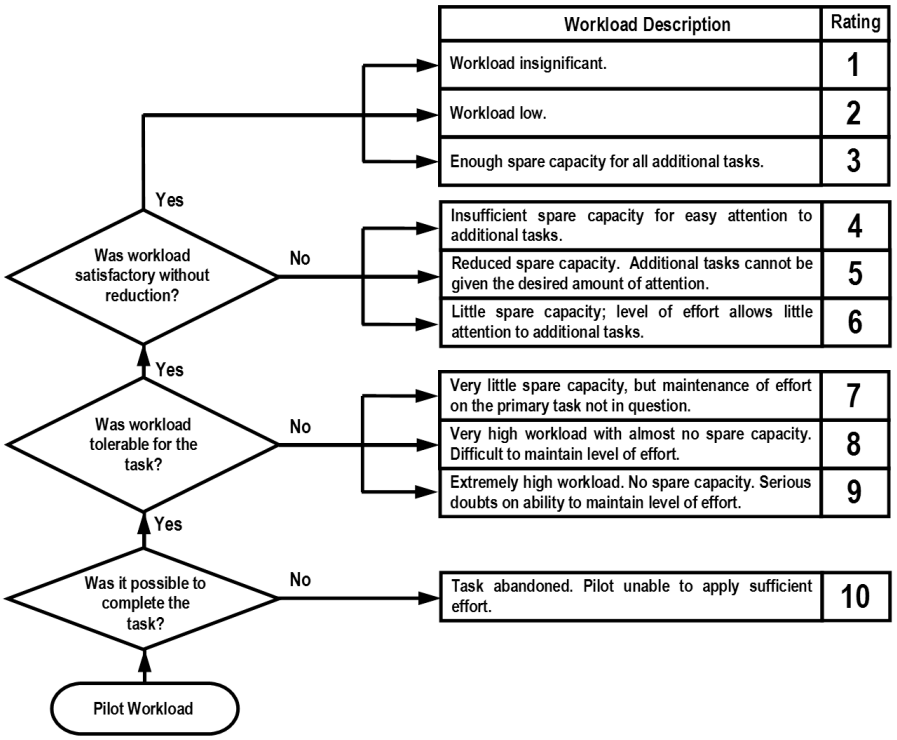

Figure 14. Bedford workload rating scale.

Although the DIPES scale has clearly been optimised for the purpose for which it was devised (i.e. qualification and clearance of SHOL envelopes), it is too coarse a scale for assessing what can often be fairly subtle variations in pilot workload, resulting from changes in simulator modelling and cueing fidelity. Therefore, in the simulator, pilot workload ratings were also taken from the 10-point Bedford workload rating scale (Fig. 14). A questionnaire study, carried out by Roscoe and Ellis during development of the scale, found that pilots naturally think in terms of spare capacity when considering workload[41]. In the Bedford scale spare capacity is defined as the pilot's ability to perform secondary tasks, such as maintaining mission awareness, monitoring aircraft systems or listening to radio communications, the primary task being to fly the aircraft through a particular manoeuvre or mission. The higher the workload generated by the primary task, the less spare capacity there is for attention to these secondary tasks.

The pilot who took part in the experiments is a highly experienced former UK Royal Navy test pilot, who has been involved in numerous FOCFT. However, when awarding workload ratings he was asked to take into consideration the capabilities of an 'average' fleet pilot, a common practice during real at-sea testing. The ability to correctly interpret subjective rating scales, and to extrapolate ratings to cover less experienced fleet pilots, are skills which are unique to the test piloting community, making the involvement of a trained test pilot essential in these types of simulator experiments. During each experiment the pilot had hardcopies of the subjective ratings scales (Figs 13 and 14) in the cockpit, so that ratings could be awarded immediately after flying each test point. An audio link to the simulator's control desk allowed pilot ratings and comments

https://doi.org/10.1017/S0001924000007545 Published online by Cambridge University Press

to be relayed to the simulator operator and these were recorded in a log file. Furthermore, video and audio recordings were made so that test points could be reviewed after the trial. The simulator software was also configured to record data files, for off-line analysis, containing various parameters relating to the pilot input, helicopter flight dynamics, ship airwake and deck motion, as well as the simulator's motion platform response.

6.3 Defining the dynamic interface environment

Each of the test points flown in the simulator required a different relative wind speed and direction. Therefore, a series of parameters had to be specified in order to completely define the conditions at the dynamic interface for each test point (i.e. ship airwake and ship motion conditions). These parameters included the wind magnitude and direction, the ship speed and heading, and the sea state. Changes in wind direction have a dramatic influence on the structure of the airwake flow field around the ship, so there is no alternative but to load a different airwake look-up table for each change in wind direction. However, the structure of the flow field does not vary greatly with changes in relative wind speed and therefore, different wind speeds may be simulated by scaling the airwake velocity components. In other words, a flow field computed for a Green 30°/40kt wind is essentially the same as one computed for a Green 30°/20kt wind, except that it is moving at twice the speed. Polsky and Bruner[3] showed that this approach is valid since the airwake solutions are Reynolds number independent over the limited range of wind speeds of interest, typically 30 to 50kt.

$$f = \frac{U_\infty S_t}{d} \qquad \ldots (1)$$

Zan[42] makes the important point that the airwake frequency content should also be shifted in proportion to wind speed. Because the large-scale disturbances in the airwake are due mainly to flow separation, it is reasonable to assume that the frequency content in the airwake will scale with wind speed and ship size, according to the Strouhal number, St, using Equation (1). This hypothesis was tested by Forrest[31] who computed, using DES, unsteady airwakes for the SFS exposed to a headwind at both 40 and 30kt. The frequency content of the airwake, measured half-way along the flight deck, at hangar height, is shown in Fig. 15. It can be seen from the power spectral density (PSD) plot that the higher wind speed contains more energy, and has higher frequency content, as predicted, and when the 40kt data is scaled to 30kt, based on a constant Strouhal number, the measured and scaled 30kt data agree reasonably well. Forrest also reported that the mean and RMS of the 30kt and 40kt airwakes also scaled with free stream velocity, confirming the findings of Polsky and Bruner[3], who found that the airwake velocity components vary linearly with the free stream velocity. For the purpose of creating an airwake simulation with the appropriate mean and unsteady characteristics, it is therefore necessary to compute an airwake at a single wind speed for each wind direction (40kt was chosen), and then scale the individual velocity components and frequency content accordingly. For example, if the desired wind speed was half that used in the original CFD simulation (i.e. 20kt), then the velocity components would be halved and the airwake time history would be replayed at half the speed, or over twice the duration of the original CFD data.

7.0 EXPERIMENT RESULTS

Three flight simulation experiments are now discussed, each one designed to address a different fidelity sensitivity issue. The first experiment was carried out to determine whether a steady airwake

https://doi.org/10.1017/S0001924000007545 Published online by Cambridge University Press

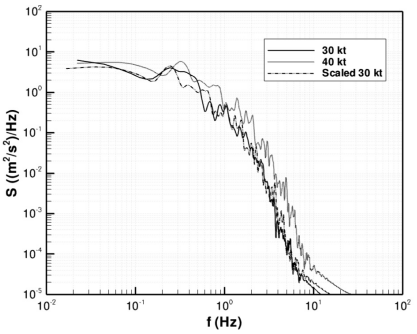

Figure 15. Power spectral density of longitudinal velocity fluctuations for scaled and un-scaled headwinds.

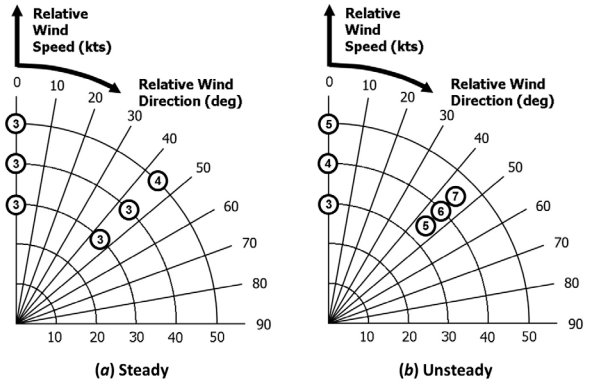

Figure 16. Bedford workload ratings for station-keeping MTE; (a) Type 23 frigate steady airwake model, (b) Type 23 frigate unsteady airwake model.

model is sufficient, or if an unsteady model is required to engender the correct levels of pilot workload. The second experiment explored whether detailed ship geometry is required, or if a simplified geometry would be acceptable, and the third experiment investigated the influence of the inlet flow conditions used in the CFD simulations on the airwake model and subsequently on the pilot's workload. Finally, the results of a simulated FOCFT will be discussed and put into operational context.

7.1 Experiment 1: Effect of steady and unsteady models

Figure 16 shows the pilot's Bedford workload ratings for the station-keeping (i.e. precision hover over the flight deck) phase of the deck landing manoeuvre, carried out with both steady and unsteady models of the Type 23 frigate airwake. The workload ratings for the steady airwake model (Fig. 16(a)) are mainly 3 ('Enough spare capacity for all additional tasks'), with one rating of 4 ('Insufficient spare capacity for easy attention to additional tasks') awarded at Green 45°/50kt, due to a requirement for large amounts of left pedal input and right bank angle. The SH-60B main rotor rotates anti-clockwise when viewed from above; the torque reaction on the airframe to the rotor drive is therefore clockwise, and the tail rotor has to pull the helicopter to the right to counter this torque. The natural still wind attitude of a helicopter with this configuration is slightly 'left wing' low. Therefore, in a strong Green wind a 'right wing' low bank angle will be required to maintain a stationary hover position. A large left pedal input will also be needed to counteract the yawing moment on the fuselage and empennage, which causes the helicopter's nose to be rotated into wind (i.e. weather-cock stability). In contrast, the pilot gave a variety of workload ratings for the station-keeping task in the presence of an unsteady airwake (Fig. 16(b)), ranging from 3 up to 7 ('Very little spare capacity, but maintenance of effort on the primary task not in question'). The pilot commented that with the steady airwake model, workload ratings were driven by deck motion (D) in the case of the headwind, and in the case of the Green 45° wind by deck motion (D), yaw control (Y) and aircraft attitude (A). However, for the unsteady airwake, a number of additional factors were identified as workload drivers, including turbulence (T), pitch/roll control (P/R), height control (H) and lateral/fore-aft positioning (L/F).

Figure 17 compares the pilot's cyclic deflections during the station-keeping task in a Green 45°/40°kt wind, with both the steady and unsteady airwake models. In Fig. 17 the cyclic deflection has been normalised between ±1 (lateral cyclic: +1 = full right, –1 = full left, longitudinal cyclic: +1

https://doi.org/10.1017/S0001924000007545 Published online by Cambridge University Press

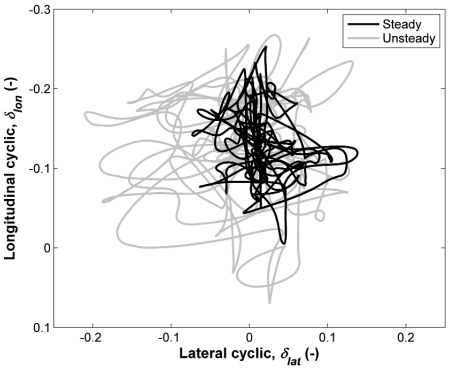

Figure 17. Pilot cyclic deflections for station-keeping MTE in a Green 45°/40kt wind.

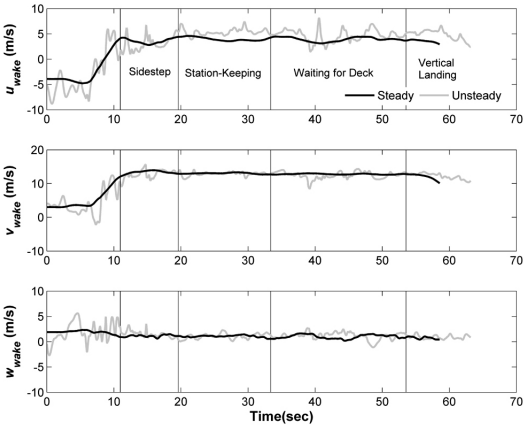

Figure 18. Airwake velocity components applied at the helicopter fuselage in a Green 45°/40kt wind.

= full aft, –1 = full forward). It can be seen that much larger control inputs were required to maintain position over the deck landing spot in the unsteady airwake, particularly in the lateral axis.

The cause of this increased workload is revealed in Fig. 18, which shows the three airwake velocity components applied at the fuselage ACP of the helicopter model. The sign convention for the airwake components follows the standard flight dynamics convention for winds, i.e. an airwake velocity is positive when it is coming from the forward and starboard side and going upward. The first vertical line in Fig. 18 is the point at which the helicopter crosses the port deck edge. The remaining vertical lines are used to split the deck landing manoeuvre into individual MTEs. It can be seen from Fig. 18 that the steady airwake model creates a largely stationary flow field, which changes only slowly as the helicopter transverses through it. However, the unsteady airwake model presents the pilot with a time-dependent disturbance rejection task, resulting in increased control activity and higher pilot workload.

7.2 Experiment 2: Effect of modelled ship geometry

Figure 19 shows the Bedford workload ratings obtained for the sidestep MTE, with unsteady airwake models of both the Simple Frigate Shape (SFS) and the Type 23 frigate. The sidestep MTE is presented here since it represents the limiting case in Green winds, where airwake turbulence

https://doi.org/10.1017/S0001924000007545 Published online by Cambridge University Press

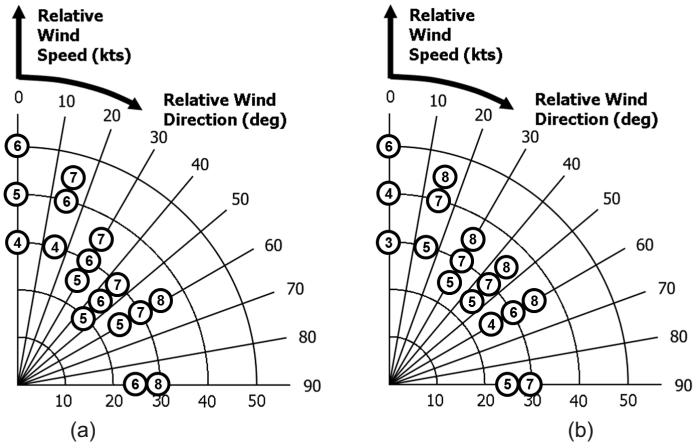

Figure 19. Bedford workload ratings for sidestep MTE; (a) Simple Frigate Shape, (b) Type 23 frigate.

will be 'swept' across the hangar face, towards the port deck-edge and into the path of the on-coming helicopter. It can be seen that for both ship geometries the workload ratings increase with relative wind speed. This is to be expected, because increases in wind speed result in turbulent fluctuations of greater magnitude and frequency in the lee of the ship's hangar. Furthermore, relative wind directions other than headwinds were awarded higher workload ratings, due to increased turbulence caused by shear layers emanating from the sides of the ship's hangar. However, it can also be seen from Fig. 19 that the workload ratings awarded for the SFS and Type 23 frigate airwakes, at comparable test points, are broadly similar (i.e. within 1 point).

On the one hand, the similarity between these two sets of results is perhaps unsurprising, because of the similarity between the fundamental bluff body geometries of the two ships. However, it has been reported by several previous studies that small differences in the modelled ship geometry can lead to significant differences in the computed airwake. For example, Zan[43] showed that the inclusion of a Phalanx Close-In Weapon System (CIWS), on top of the starboard corner of the hangar on a Canadian patrol frigate model, substantially affected the flow topology over the flight deck. Likewise, significant differences exist in the airflow around the simplified SFS and the more complex Type 23 frigate models. For example, lower velocities are observed over the Type 23 flight deck, mainly because the Type 23 model contains several realistic geometric features including masts, weapons, equipment and radars, which slow the free stream flow and break-up large scale vortices. In contrast, the SFS model is practically clean apart from a single funnel-type arrangement on top of the hangar.

One area where there are significant differences between the SFS and Type 23 flow fields is for Green 45° winds. Figure 20 shows mean path-lines in a portion of a Green 45° airwake that flows around the hangar edge and across the flight deck. It can be seen that the notch in the side of the Type 23 hangar generates a streamwise vortex over the flight deck; given the strength and size of this flow feature it will have a significant effect on the aerodynamic loads imparted on the helicopter during the landing manoeuvre. It should also be noted that both of the flow features shown in Fig. 20 are unsteady. The fact that the hangar of the Type 23 does not extend across the full width of the flight deck also affects the air flow.

In summary, although there are strong similarities in the pilot's workload ratings, critical wind azimuths do exist where relatively small geometric features create significantly different flow fields. The exact amount of geometric fidelity required to model a ship's airwake for accurate prediction of

https://doi.org/10.1017/S0001924000007545 Published online by Cambridge University Press

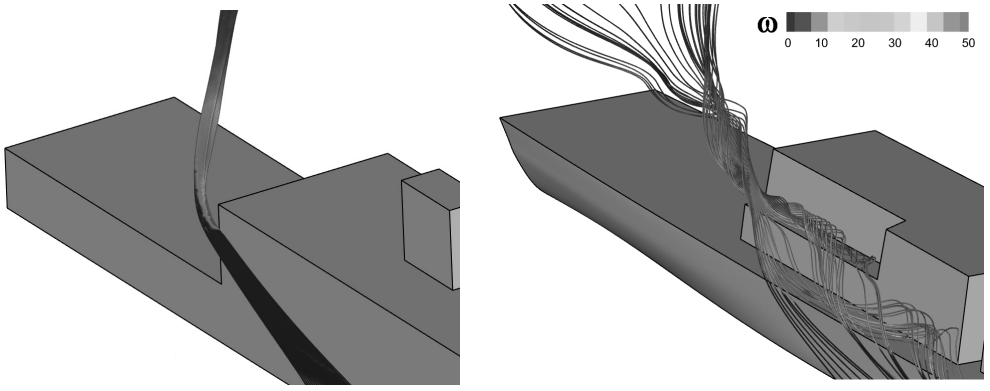

(a) (b)

Figure 20. Flow field for a Green 45° wind path-lines coloured by vorticity magnitude; (a) Simple Frigate Shape, (b) Type 23 frigate.

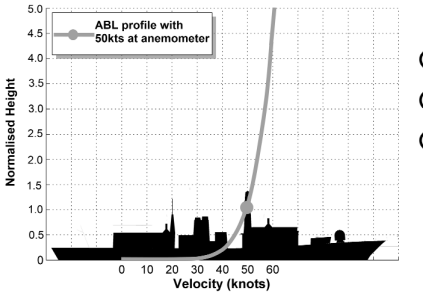

Figure 21. Air-sea Boundary-Layer velocity profile with 50kt at the ship's anemometer height.

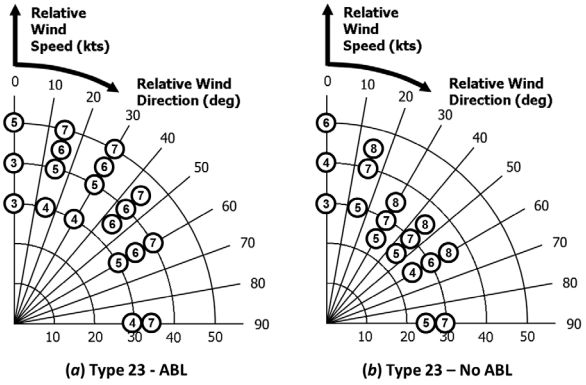

Figure 22. Bedford workload ratings for sidestep MTE; (a) Type 23 with ABL inlet velocity profile, (b) Type 23 with uniform inlet velocity profile.

the SHOL remains a largely unanswered question. The potential savings to be gained from reducing the complexity of the ship model, and therefore, the model development and processing time, could be considerable and will no doubt provide a fruitful area for future research. However, the realisation of any savings in this area must first be weighed against the fidelity requirements of the simulation. For example, a simplified ship model may well be acceptable for pilot training and familiarisation purposes, but a highly detailed model will no doubt be necessary for predicting SHOL envelopes.

7.3 Experiment 3: Effect of air-sea boundary-layer inlet profile

In the CFD simulations the inlet flow conditions have to be defined at the up-stream boundary of the simulation domain, ahead of the ship. There are essentially two possible choices for the inlet profile – a uniform profile, which assumes that the free stream wind velocity is the same at any height; or one which models the Air-sea Boundary Layer (ABL), where the wind speed reduces close to the sea due to surface drag[44] (Fig. 21).

The Bedford workload ratings obtained for the sidestep MTE, using unsteady airwake models of the Type 23 frigate with both types of inlet profiles, are shown in Fig. 22. It can be seen that

https://doi.org/10.1017/S0001924000007545 Published online by Cambridge University Press

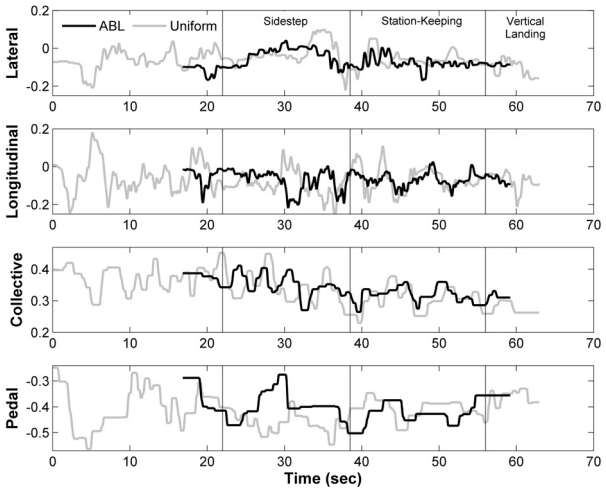

Figure 23. Pilot control activity during deck landings in a Green 30°/30kt wind.

there are considerable differences in pilot workload between the two airwake models, particularly for wind azimuths of Green 15° and greater. Note that the relative wind speeds presented in Fig. 22 are the wind speeds measured at the ship's reference anemometer. The actual wind speed at flight deck height will be lower in the case of the ABL profile as shown in Fig. 21. For example, the wind speed at flight deck height will be approximately 82% of the anemometer reading, while at hangar height it will be approximately 92% of the anemometer reading.

Figure 23 presents the pilot's control activity during deck landings in a Green 30°/30kt wind and shows that performing the deck landing task with a uniform inlet profile is clearly more challenging than with an ABL inlet profile. The vertical lines in Fig. 23 coincide with the pilot commencing the sidestep, the beginning of the station-keeping MTE and the beginning of the vertical landing. With the uniform inlet velocity profile the pilot takes more than twenty seconds to stabilise alongside the ship, after initial release of the simulation. During this period the pilot's control activity is considerable, particularly the longitudinal cyclic, collective and pedal inputs. Generally speaking, pilot control activity is higher throughout the whole manoeuvre with the uniform inlet profile, compared to the ABL inlet profile.

The trajectory of the helicopter's main rotor hub is shown in Fig. 24 and it is clear that, with the uniform inlet profile, the pilot experiences severe difficulty in obtaining a stable hover position alongside the ship. The marked disturbances experienced alongside the ship with the uniform inlet profile were described by the pilot as 'uncomfortable' and 'more like those you'd expect with a much stronger wind'. Once the helicopter is over the deck landing spot, then airwake turbulence diminishes in Green winds, and station-keeping accuracy is good. These observations are confirmed by test pilot comments i.e. 'Marked disturbances at start of the translation', 'Lots of collective [activity] required', 'Fine when you're over the spot'.

Figure 25 shows the DIPES ratings for each of the deck landings and the corresponding SHOL envelopes. The SHOL envelope derived from the uniform inlet profile ratings (No ABL) is severely restricted, compared to the ABL inlet profile. In fact, many of the wind conditions which fall outside of the uniform inlet profile SHOL are so critical to embarked helicopter operations, that the test pilot suggested that in reality an alternative approach technique would be recommended for those conditions (i.e. into wind landings) so that they could still be achieved.

https://doi.org/10.1017/S0001924000007545 Published online by Cambridge University Press

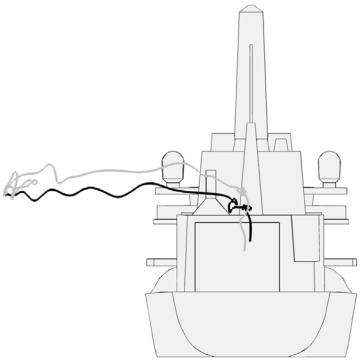

Figure 24. Helicopter's main rotor hub trajectory during deck landings in a Green 30°/30kt wind (black – ABL inlet profile, grey – uniform inlet profile).

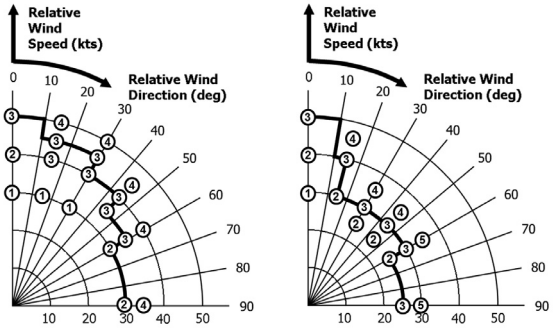

(a) Type 23 – ABL (b) Type 23 – No ABL

Figure 25. DIPES ratings and SHOL envelope; (a) Type 23 with an ABL inlet profile, (b) Type 23 with a uniform inlet profile.

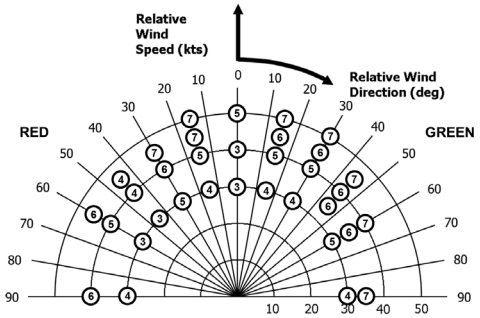

Figure 26. Bedford workload ratings for sidestep MTE.

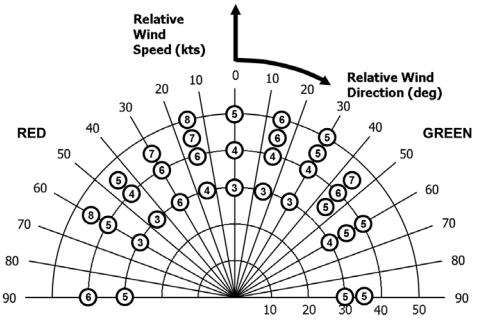

Figure 27. Bedford workload ratings for station-keeping MTE.

The difference in pilot workload with and without an ABL inlet profile is an important finding in terms of simulation fidelity, since it has been shown that by omitting the ABL a very restrictive SHOL envelope is predicted. Based on a review of past studies, reported in the open literature, the importance of modelling realistic inlet conditions does not appear to have been fully appreciated. For example, out of several airwake modelling papers reviewed, only a few have specifically stated that an ABL inlet profile was included in their models. It is hoped that these results will help highlight the importance of proper modelling of the ABL and encourage modellers to ensure that appropriate inlet conditions are incorporated into future airwake simulations, particularly those whose data are destined for integration into flight simulators. The practice of including an ABL profile in CFD models is entirely consistent with those employed in structural engineering applications for modelling tall buildings and off-shore structures.

7.4 Simulated first-of-class flying trials

Finally, simulated FOCFT were conducted using the 'highest' fidelity airwake models available (i.e. unsteady, using detailed ship geometry with an ABL inlet profile). The Bedford workload ratings for the sidestep and station-keeping MTEs are shown in Figs 26 and 27 respectively, and the DIPES ratings and predicted SHOL are shown in Fig. 28.

https://doi.org/10.1017/S0001924000007545 Published online by Cambridge University Press

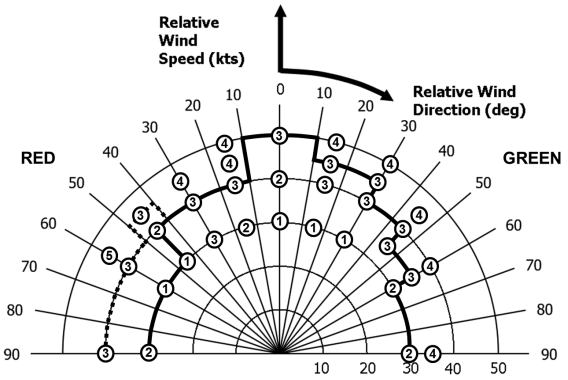

Figure 28. Type 23 frigate/SH-60B Seahawk DIPES ratings and predicted SHOL.

During deck landings with the wind from ahead, turbulence will mainly be experienced in the lee of the ship's hangar. Therefore, the station-keeping MTE will present the most demanding task for headwinds. For Green winds between 30° and 60° the chief factor determining the SHOL boundaries, will be the turbulence experienced while hovering alongside the ship. Therefore, the translation across the deck (sidestep) will be the most demanding task. Once in position behind the ship's hangar then flow conditions will be close to free stream and the turbulence will diminish. For Red winds between 30° and 60° the opposite is true. Disturbances alongside the ship will be minimal, but the pilot will experience strong turbulence as the helicopter passes the edge of the deck and while hovering over the landing spot. In beam wind conditions, between 60° and 90°, on both sides of the SHOL, the critical factor will be pedal authority and the SHOL will normally be limited by the aircraft's maximum lateral velocity. In Fig. 28 the dotted lines represent areas of the SHOL that might be expanded if only DIPES ratings (pilot workload) were considered. For beam winds between 60° and 90° a maximum lateral velocity of 30kt has been assumed, which places these areas outside of the SHOL envelope. Unfortunately, it is not possible to validate these results, since no comparable SHOL exists for clearing SH-60B operations aboard the Type 23 frigate, since these operations are not routinely conducted by the Royal Navy. The operation of helicopters from other nations onto Royal Navy ships is termed 'cross operating' or 'cross decking' and is cleared for only a very restricted set of wind and ship motion conditions[9].

8.0 LIMITATIONS OF CURRENT REAL-TIME ANALYSIS

The research described in this paper was purely focussed on improving the fidelity of real-time helicopter-ship dynamic interface simulations. However, it is worthwhile reflecting on the limitations of the current real-time analysis and suggesting areas where further research, or increases in computing power, may contribute to significant improvements in the fidelity of future simulations. A truly high-fidelity simulation of the helicopter-ship dynamic interface is one where the influence of the ship's motion on the airwake, as well as the coupling between the rotor downwash and the airwake is modelled. For example, while hovering above the ship's deck at low wind speeds the helicopters main rotor downwash will pass over the fuselage, impinge on the flight deck, then move along the deck and up the hangar face, and become re-ingested into the rotor. This effect is not captured by the current real-time airwake model, since the airwake was calculated without the presence of the helicopter fuselage or main rotor. The exact impact of this effect will

https://doi.org/10.1017/S0001924000007545 Published online by Cambridge University Press

of course be dependent on the distance of the rotor from the hangar and on the dimensions of the hangar[7]. Furthermore, the ship's airwake will contain significant velocity gradients over the region occupied by the helicopter's fuselage therefore, the use of aerodynamic load coefficients determined from uniform flow wind-tunnel data, as is the case for the conventional flight dynamics model used in these experiments, may be questionable.

Hodge *et al*[4] attempted to improve this situation by modelling unsteady fuselage loads using data tables derived from wind-tunnel experiments of a fully-coupled helicopter-ship dynamic interface in their real-time simulations. The results showed a difference in pilot's subject ratings and measured control activity for a Green 30° wind but not for a headwind, compared with the conventional method of fuselage loads modelling. Polsky and Naylor[45] found that a real-time piloted simulation of a fixed-wing F/A-18 C/D aircraft landing on an aircraft carrier, employing the one-way coupling method, produced unrealistic lift forces on the aircraft as it flew over the stern of the ship, causing the aircraft to 'float' over the ideal touchdown point. One potential cause of this phenomenon is the one-way coupling assumption and further work has been carried out, using a fully-coupled CFD simulation of the aircraft and ship, to establish the influence of aerodynamic coupling between the aircraft and ship flowfields[46]. In the same piloted simulations a short study was conducted to examine the sensitivity of touchdown dispersion (a key metric for fixed-wing carrier landings) to the grid spacing used in the simulator's airwake look-up tables and the sampling frequency used for exporting the airwake data. Two grids were used with spatial resolutions of 5ft and 2·5ft, and the airwake data was exported at frequencies of 10Hz and 20Hz. It was found that refining the grid spacing to 2·5ft, whilst keeping the export frequency at 10Hz, produced a similar reduction in touchdown dispersion to that which occurred when the export frequency was increased to 20Hz at the coarser grid spacing of 5ft. However, increasing the export frequency to 20Hz and refining the grid spacing to 2·5ft together, showed no improvement in touchdown dispersion beyond doing one or the other alone. Further work is still required to understand the implications of these results. Moreover, the choice of airwake sampling frequency may be even more important in helicopter-ship simulations due to the harmonic nature of the helicopter's main rotor system.

Further areas where improvements to the current state-of-the-art in helicopter-ship dynamic interface simulations are warranted include, the modelling of aeroelastic blade characteristics, engine response to funnel efflux ingestion, main rotor and tail rotor interactions, over-the-deck 'ground' effects, landing gear-deck interaction dynamics and, for large ships, the aerodynamic interactions between multiple aircraft. The future goal is to develop technology to allow fully-coupled real-time simulations where the rotor downwash, ship airwake and ship motion interact with each other in a realistic manner. However, the computing power required to perform such calculations in real-time, means that this capability will be 'out-of-reach' of piloted simulations for some years to come. The current research represents a significant increase in fidelity beyond current real-time helicopter-ship simulations. Any simplifying assumptions, such as the one-way coupling assumption, and the choice of airwake sampling frequency and spatial resolution, have been made pragmatically based on the available real-time bandwidth, data storage capacity and processing power limitations.

9.0 DISCUSSION

The current research into simulation fidelity criteria for dynamic interface simulations is timely for two reasons. First, the ready availability of PC and simulation technology; including visual image generators, projectors, computing clusters and electric motion systems, has opened-up the

https://doi.org/10.1017/S0001924000007545 Published online by Cambridge University Press

potential for much improved levels of fidelity at reduced costs[47]. The key to unlocking this increased fidelity is however, through improvements to the underlying physics modelling (e.g. ship airwake and flight dynamics modelling) and a deeper understanding of the influence of the simulator cueing environment on pilot behaviour[48]. Second, there are a number of current industry programmes in the UK that could directly benefit from this research. Today's defence budgets are under increasing pressure and procurement programmes now rely heavily on modelling and simulation for design, verification and qualification of products. An increasing reliance on simulation, together with a rising demand for high-fidelity simulators for pilot training purposes, has brought into sharp focus the need for simulation fidelity criteria and modelling guidelines. This is particularly true in cases were ship and aircraft designs are evolving concurrently[49], and for operations involving Maritime Uninhabited Air-Vehicles (MUAVs).

10.0 CONCLUSIONS

An aircraft-ship dynamic interface simulation has been developed at the University of Liverpool based on an existing rotorcraft flight simulator. The simulation was populated with a range of models including a helicopter flight dynamics model, ship airwake and motion models, and visual models of the ship and ocean surface. The purpose of developing the simulation was to conduct the fidelity sensitivity experiments described in this paper. These experiments explored some fundamental questions from the perspective of simulation fidelity and the following conclusions are drawn:

1. The first question was to determine if an unsteady airwake was required, or, if a steady airwake could provide the desired level of fidelity. The results showed that pilot workload increased significantly with the introduction of an unsteady airwake, and furthermore, that the source of pilot workload changed from predominately deck motion with the steady airwake, to turbulence with the unsteady airwake. This result confirms the importance of an unsteady airwake for correctly modelling pilot workload in the simulator.
2. Pilot workload ratings taken with unsteady airwake models of the SFS and the more realistic Type 23 frigate ship geometries were broadly similar. This result suggests that simplified ship models may be acceptable for developing airwake simulations for some applications (e.g. pilot training and familiarisation). However, some critical wind azimuths do exist where relatively small differences in ship geometry influenced the pilot's workload noticeably. Therefore, detailed ship models will still be required for the purposes of predicting safe operating envelopes in a simulator.
3. The difference in pilot workload experienced both with and without an inlet velocity profile approximating the ABL, was an important finding. Without an ABL inlet profile, disturbances alongside the ship were described as 'uncomfortable' and resulted in considerable pilot workload. The inclusion of the ABL profile reduced the velocity of the flow over the ship, which significantly reduced pilot workload and resulted in a less restricted SHOL. It is strongly recommended that appropriate inlet conditions are included in all future ship airwake models.
4. Finally, simulated FOCFT were conducted using the 'highest' fidelity airwake models (i.e. unsteady, using detailed ship geometry with an ABL inlet profile). DIPES ratings were taken and a SHOL was derived for the Type 23 frigate and SH-60B Seahawk helicopter. It was not possible to validate the resulting SHOL due to a lack of appropriate 'real-world' data, but a methodology for collecting SHOL data using a flight simulator was developed and shows promise.

https://doi.org/10.1017/S0001924000007545 Published online by Cambridge University Press

ACKNOWLEDGEMENTS

This research was conducted as part of a part-time PhD programme followed by the first author. The first author wishes to thank his employers BAE Systems, for allowing him to undertake the research, particularly Mr. Mike Southworth, Business Development Manager of the Simulation Department at Warton, for his continued support and encouragement. The valuable assistance of Dr Mark White and Dr Philip Perfect of the Flight Science and Technology Research group at the University of Liverpool is gratefully acknowledged. The SFS2 validation data was derived by the National Research Council Canada, and provided under the The Technical Cooperation Program (TTCP). The Type 23 frigate validation data was provided by DSTL. This work would not have been a success without the expert skill, guidance and knowledge of our professional test pilot, Mr Andy Berryman.

REFERENCES

1. WOODFIELD, A.A. and TOMLINSON, B.N. Ship Airwakes – A new Generic Model for Piloted Simulation, AGARD-CP-577, AGARD Flight Vehicle Integration Panel Symposium on 'Flight Simulation Where are the Challenges?', Braunschweig, Germany, May 1995.
2. WILKINSON, C.H., ZAN, S.J. GILBERT, N.E. and FUNK, J.D. Modeling and Simulation of Ship Air Wakes for Helicopter Operations – A Collaborative Venture, presented at the RTO AVT Symposium on 'Fluid Dynamics Problems of Vehicles Operating near or in the Air-Sea Interface', Amsterdam, Netherlands, October 1998.
3. POLSKY, S.A. and BRUNER, C.W.S. Time-Accurate Computational Simulation of an LHA Ship Airwake, AIAA Paper No. 2000-4126, 18th Applied Aerodynamics Conference, Denver, Colorado, USA, August 2000.
4. HODGE, S.J., ZAN, S.J., ROPER, D.M., PADFIELD, G.D. and OWEN, I. Time-Accurate ship airwake and unsteady aerodynamic loads modeling for maritime helicopter simulation, *J the American Helicopter Society*, April 2009, **54**.
5. PADFIELD, G.D. The making of helicopter flying qualities; A requirements perspective, *Aeronaut J*, December 1998, **102**, (1018).
6. TATE, S.J. A Dynamic Challenge: Helicopter/Ship Interface Simulation – Development, Integration and Application, AGARD-CP-577, AGARD Flight Vehicle Integration Panel Symposium on 'Flight Simulation Where are the Challenges?', Braunschweig, Germany, May 1995.
7. LUMSDEN, B. and PADFIELD, G.D. Challenges at the Helicopter-Ship Dynamic Interface, Military Aerospace Technologies – Fitec '98, IMechE Conference Transactions, Institute of Mechanical Engineers, Wiley, UK, 1998.
8. FINLAY, B.A. Ship Helicopter Operating Limit Testing – Past, Present and Future, RAeS Rotorcraft Group Conference on 'Helicopter Operations in the Maritime Environment', London, UK, March 2001.
9. HOENCAMP, A. An Overview of SHOL Testing Within The Royal Netherlands Navy, 35th European Rotorcraft Forum, Hamburg, Germany, 2009.
10. BARNES, A. Compromise between Accuracy and Realism in Flight Simulation, AIAA Paper No. 1991-2920, August 1991.
11. REHMANN, A.J. A Handbook of Flight Simulation Fidelity Requirements for Human Factors Research, DOT/FAA/CT-TN95/46, US Department of Transportation, Federal Aviation Administration, December 1995.
12. HESS, R.A. and SIWAKOSIT, W. Assessment of simulation fidelity in multiaxis tasks including visual cue quality, *J Aircr*, July-August 2000, **38**, (4).
13. BRAY, R.S. Visual and Motion Cueing in Helicopter Simulation, AGARD-CP-408, AGARD Flight Mechanics Symposium on 'Flight Simulation', Cambridge, UK, October 1985.
14. Anon, Manual of Criteria for the Qualification of Flight Simulator Training Devices, Doc 9625, International Civil Aviation Organization, Third Edition, 2009.
15. WILKINSON, C.H. ROSCOE, M.F. and VANDERVLIET, G.M. Determining Fidelity Standards for the Shipboard Launch and Recovery Task, AIAA Paper No. 2001-4062, AIAA Modeling and Simulation Technologies Conference, Montreal, Canada, August 2001.

16. REDDY, W. V-22 Simulator Evaluation for Shipboard Operations, RAeS Rotorcraft Group Conference on 'Rotorcraft Simulation', London, UK, May 1994.
17. ADVANI, S.K. and WILKINSON, C.H. Dynamic Interface Modelling and Simulation – A Unique Challenge, RAeS Flight Simulation Group Conference on 'The Challenge in Achieving Realistic Training in Advanced Rotorcraft Simulators', London, UK, November 2001.
18. BUNNELL, J.W. An Integrated Time-Varying Airwake in a UH-60 Black Hawk Shipboard Landing Simulation, AIAA Paper No. 2001-4056, AIAA Modeling and Simulation Technologies Conference, Montreal, Canada, August 2001.
19. HOWLETT, J.J. UH-60A Black Hawk Engineering Simulation Program: Volume I – Mathematical Model, NASA-CR-166309, December 1981.
20. COX, I. TURNER, G. and DUNCAN, J. Applying a Networked Architecture to the Merlin Helicopter Simulator, RAeS Flight Simulation Group Conference on 'Multi Role and Networked Simulation: Networking of Simulators – For Better or Worse?', London, UK, May 2005.
21. BRIDGES, D.O., HORN, J. F., ALPMAN, E. and LONG, L.N. Coupled Flight Dynamics and CFD Analysis of Pilot Workload in Ship Airwakes, AIAA Paper No. 2007-6485, AIAA Atmospheric Flight Mechanics Conference, Hilton Head, South Carolina, USA, August 2007.
22. WHITE, M.D., PERFECT, P., PADFIELD, G.D., GUBBELS, A.W. and BERRYMAN, A. Acceptance Testing of a Rotorcraft Flight Simulator for Research and Teaching: The Importance of Unified Metrics, 35th European Rotorcraft Forum, Hamburg, Germany, September 2009.
23. HODGE, S.J. PERFECT, P., PADFIELD, G.D. and WHITE, M.D. Optimising the Vestibular Cues Available from a Short Stroke Hexapod Motion Platform, American Helicopter Society 67th Annual Forum, Virginia Beach, Virginia, USA, May 2011.
24. DUVAL, R.W. A Real-Time Multi-Body Dynamics Architecture for Rotorcraft Simulation, RAeS Flight Simulation Group Conference on 'The Challenge in Achieving Realistic Training in Advanced Rotorcraft Simulators', London, UK, November 2001.
25. MANIMALA, B.J. WALKER, D.J. PADFIELD, G.D. VOSKUIJL, M. and GUBBELS, A.W. Rotorcraft Simulation modelling and validation for control law design, *Aeronaut J*, February 2007, **111**, (1116).
26. BECK, C.P. and FUNK, J.D. Development and Validation of a Seahawk Blade Element Helicopter Model in Support of Rotorcraft Shipboard Operations, RAeS Rotorcraft Group Conference on 'Rotorcraft Simulation', London, UK, May 1994.
27. PADFIELD, G.D. *Helicopter Flight Dynamics: The Theory and Application of Flying Qualities and Simulation Modelling*, 2nd ed, Blackwell Publishing, Oxford, UK, 2007.
28. BOGSTAD, M.C., HABASHI, W.G., AKEL, I., AIT-ALI-YAHIA, D., GIAMMOAS, N. and LONGO, V. Computational-Fluid-Dynamics based advanced ship-airwake database for helicopter flight simulators, *J Aircr*, **39**, (5), September-October 2002.
29. ROPER, D., OWEN, I., PADFIELD, G.D. and HODGE, S. J. Integrating CFD and piloted simulation to quantify ship-helicopter operating limits, *Aeronaut J*, July 2006, **110**, (1109).
30. FORREST, J.S., OWEN, I., PADFIELD, G.D. and HODGE, S.J. Detached-Eddy Simulation of Ship Airwake for Piloted Helicopter Flight Simulation, 1st International Aerospace CFD Conference, Paris, France, June 2007.
31. FORREST, J.S. and OWEN, I. An investigation of ship airwakes using detached-eddy simulation, *Computers & Fluids*, April 2010, **39**, (4).
32. CARICO, D. Rotorcraft Shipboard Flight Testing Analytic Options, IEEE Aerospace Conference Proceedings, 5, March 2004.
33. PADFIELD, G.D. Handling Qualities for Maritime Helicopter Operations, American Helicopter Society 53rd Annual Forum, Virginia Beach, Virginia, May 1997.
34. HODGE, S.J. Validation of Shipborne Visual Landing Aids Through Piloted Simulation, RAeS Flight Simulation Group conference on 'Simulation of On-board Systems', November 2004, London, UK.
35. CSANADY, G.T. *Air-sea Interaction: Laws and Mechanisms*, Cambridge University Press, Cambridge, UK, 2001.
36. LACHMAN, L.M. An Open Programming Architecture for Modelling Ocean Waves, IMAGE 2007 Conference, Scottsdale, Arizona, USA, July 2007.
37. BICKERSTAFF, I.H. Portrait of Landscape: A Visualisation Solution for Military Aircraft Development, IMAGE 1998 Conference, Scottsdale, Arizona, USA, August 1998.
38. SPENCE, G.T., LE MOIGNE, A., ALLERTON, D.J. and QIN, N. Wake Vortex model for real-time flight simulation based on large eddy simulation, *J Aircr*, **44**, 2 March 2007.

39. Anon, Aeronautical Design Standard, Performance, Specification, Handling Qualities Requirements for Military Rotorcraft, ADS-33E-PRF, U.S Army Aviation and Missile Command, March 2000.
40. SMITH, J.R. and MITCHELL, W.S. Aircraft/Ship Interface Problems – The U.S. Navy's Program, AIAA Paper No. 74-305, AIAA/SNAME Advanced Marine Vehicles Conference, San Diego, California, USA, February 1974.
41. ROSCOE, A.H. and ELLIS, G.A. A Subjective Ratings Scale for Assessing Pilot Workload in Flight: A Decade of Practical Use, RAE Technical Report, RAE-TR-90019, 1990.
42. ZAN, S.J. On Aerodynamic Modelling and Simulation of the Dynamic Interface, Proceedings of the Institute of Mechanical Engineers, Part G: *J Aerospace Engineering*, 2005, **219**, (5).
43. ZAN, S.J., SYMS, G.F. and CHENEY, B.T. Analysis of Patrol Frigate Air Wake, presented at the RTO AVT Symposium on 'Fluid Dynamics Problems of Vehicles Operating near or in the Air-Sea Interface', Amsterdam, Netherlands, October 1998.
44. MAKIN, V.K., KUDRYAVTSEV, V.N. and MASTENBROEK, C. Drag of the sea surface, *Boundary Layer Meteorology*, **73**, 1995.
45. POLSKY, S. and NAYLOR, S. CVN Airwake Modelling and Integration: Initial Steps in Creation and Implementation of a Virtual Burble Model for F-18 Carrier Landing Simulation, AIAA Paper 2005-6298, AIAA Modeling and Simulation Technologies Conference, San Francisco, California, August 2005.
46. POLSKY, S. Progress Towards Modeling Ship/Aircraft Dynamic Interface, IEEE HPCMP Users Group Conference Proceedings, 2006.
47. HODGE, S.J., PADFIELD, G.D. and SOUTHWORTH, M.R. Helicopter-Ship Dynamic Interface Simulation: Fidelity at Low-Cost, RAeS Flight Simulation Group Conference on 'Cutting Costs in Flight Simulation – Balancing Quality and Capability', London, UK, November 2006.
48. HODGE, S.J., FORREST, J.S., PADFIELD, G.D. and WHITE, M.D. Determining Fidelity Standards for Maritime Rotorcraft Simulation, RAeS Rotorcraft Group Conference on 'Maritime Operations of Rotorcraft', London, UK, June 2008.
49. HODGE, S.J. and WILSON, P.N. Operating JSF from CVF: The Reality of Simulation, Biennial International Powered Lift Conference, London, UK, June 2009.